Plasmids Mediating Quinolone Resistance

Subjects: Microbiology

Contributor: Hongyang Zhang , Mingding Chang , Xiaochen Zhang , Peiyan Cai , Yixin Dai , Tongzhen Song , Zhenzhou Wu , Haijin Xu , Mingqiang Qiao

Plasmid-mediated quinolone resistance (PMQR) remains one of the main mechanisms of bacterial quinolone resistance and plays an important role in the transmission of antibiotic resistance genes (ARGs). The two novel plasmids, p3M-2A and p3M-2B, which mediate quinolone resistance in *Proteus vulgaris* strain 3M (P3M) were identified. Of these, only p3M-2B appeared to be a *qnrD*-carrying plasmid. Both p3M-2A and p3M-2B could be transferred into *Escherichia coli*, and the latter caused a twofold change in ciprofloxacin resistance, according to the measured minimum inhibitory concentration (MIC). Plasmid curing/complementation and qRT-PCR results showed that p3M-2A can directly regulate the expression of *qnrD* in p3M-2B under treatment with ciprofloxacin, in which process, *ORF1* was found to play an important role. Sequence alignments and phylogenetic analysis revealed the evolutionary relationships of all reported *qnrD*-carrying plasmids and showed that *ORF1–4* in p3M-2B is the most conserved backbone for the normal function of qnrD-carrying plasmids. The identified direct repeats (DR) suggested that, from an evolutionary perspective, p3M-2B may have originated from the 2683-bp *qnrD*-carrying plasmid and may increase the possibility of plasmid recombination and then of *qnrD* transfer. To the best of our knowledge, this is the first identification of a novel *qnrD*-carrying plasmid isolated from a *P. vulgaris* strain of shrimp origin and a plasmid that plays a regulatory role in *qnrD* expression. This study also sheds new light on plasmid evolution and on the mechanism of horizontal transfer of ARGs encoded by plasmids.

quinolone resistance | Proteus vulgaris | qnrD-carrying plasmids | qnrD expression | direct repeats | homologous recombination

1. Effect of p3M-2A on the Expression of qnrD in p3M-2B

The plasmids p3M-2A and p3M-2B of P3M were sequenced, and their total length resulted to be 2656 bp and 5903 bp, respectively (Figure 1A). No resistance genes were present in p3M-2A, while p3M-2B carried *qnrD*. In this study, we found a certain correlation between these two plasmids—a large portion of the entire p3M-2A sequence shared a relatively high sequence identity (>89%) with *ORF2–ORF4* and their intergenic regions of p3M-2B, implying that these two plasmids may originate from the same plasmid backbone (Figure 1B). Besides, we did not find any sequence with high identity withMicroorganisms *ORF1* of p3M-2A in the database, and the same was observed for *ORF5* of p3M-2B.

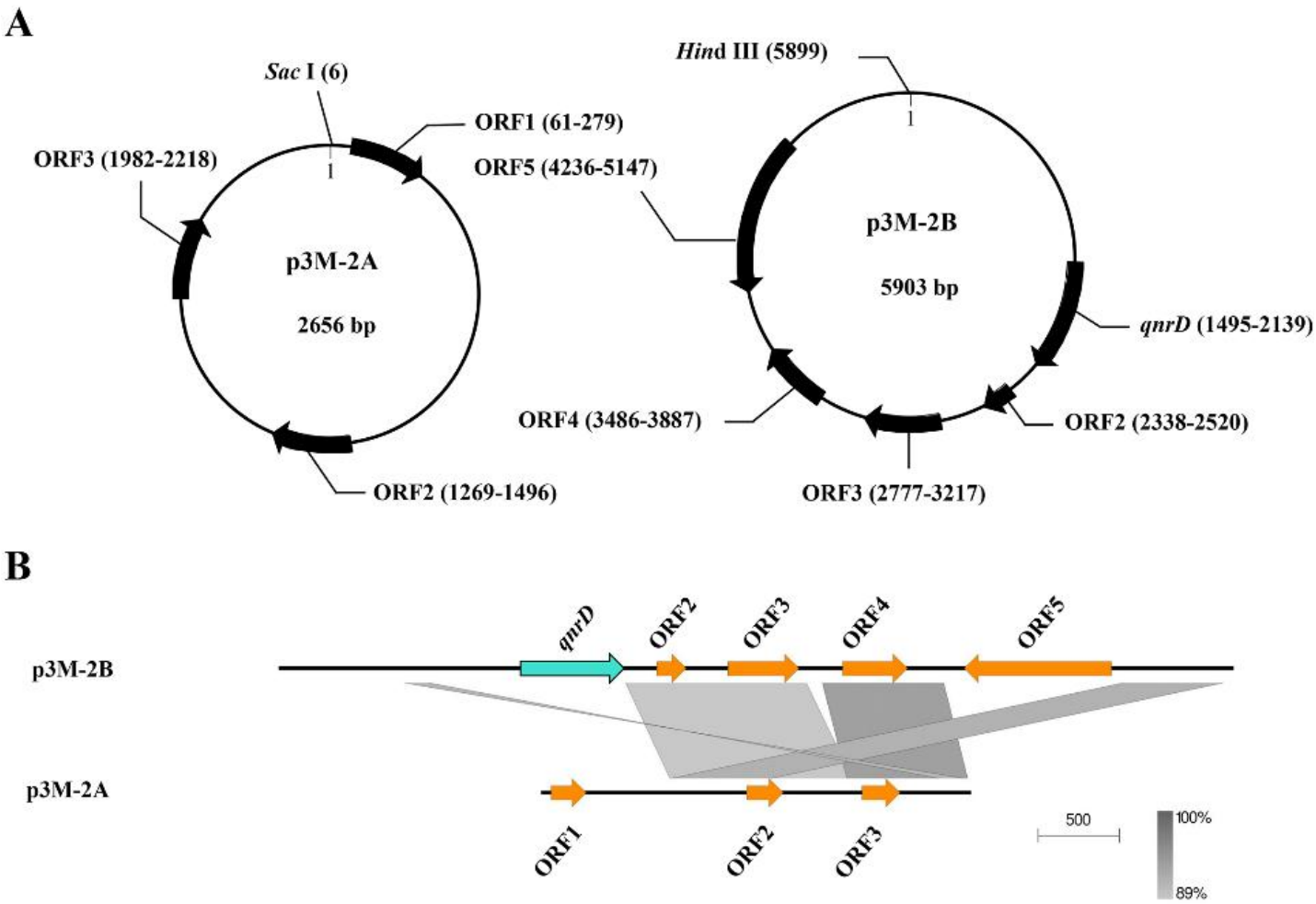

Figure 1. Graphical maps (**A**) and comparison of the structures (**B**) of p3M-2A and p3M-2B. The grey and dark shading in (b) indicates common regions between the plasmids.

In order to verify the function of p3M-2A and p3M-2B, different plasmid deletion strains of P3M were generated: P3M-Δ2A (p3M-2A elimination), P3M-Δ2B (p3M-2B elimination), and P3M-Δ2A2B (p3M-2A and p3M-2B elimination). In addition, p3M-2A and p3M-2B were transferred into *E. coli* DH5α separately or simultaneously to generate transformants with different plasmids: *E. coli* DH5α-2A (transformant containing p3M-2A), *E. coli* DH5α-2B (transformant containing p3M-2B), and *E. coli* DH5α-2A2B (transformant containing p3M-2A and p3M-2B). The ciprofloxacin MIC of these strains were determined. As shown in Table 2, ciprofloxacin resistance was decreased in P3M-Δ2A and P3M-Δ2B compared with P3M. Likewise, the resistance to ciprofloxacin was also reduced in *E. coli* DH5α transformants containing only p3M-2A or p3M-2B compared with *E. coli* DH5α-2A2B. These results showed that the presence of both plasmids caused an eight- or four-fold change in the ciprofloxacin resistance of P3M and *E. coli* DH5α-2A2B compared with the plasmid-free strains, respectively. In addition, we found that the ciprofloxacin resistance of P3M-Δ2A and *E. coli* DH5α-2B strains containing only p3M-2B increased by four times or two times, respectively, while p3M-2A did not contribute to strain resistance. These results indicated that the two plasmids played synergistic roles in improving strain resistance to ciprofloxacin, and p3M-2B had a more obvious promoting effect. It is worth noting that, despite the absence of *qnrD*, p3M-2A still played a

specific role in improving
the quinolone resistance of the bacteria tested.

Table 2. Determination of the MIC of ciprofloxacin in different transformants with respect to the parental strains.

Strains	MIC to Ciprofloxacin (mg/L) [a]
P3M	1
P3M-Δ2A	0.5
P3M-Δ2B	0.125
P3M-Δ2AΔ2B	0.125
E. coli DH5α-2A2B	0.125
E. coli DH5α-2B	0.06
E. coli DH5α-2A	0.03
E. coli DH5α	0.03

[a] All MIC determinations were performed by broth microdilution assays according to CLSI standards.

To confirm the function of p3M-2A, we carried out spot growth assays to test the effect of the absence of p3M-2A on the stability of p3M-2B. After subcultured for 100 generations, P3M-Δ2A and DH5α-2B were able to preserve the ciprofloxacin-resistant phenotype in the presence of 0.25 mg/L and 0.05 mg/L of ciprofloxacin, respectively (Figure 2A,B), showing that p3M-2B could replicate and function independently and the absence of p3M-2A had no effect on the stability of p3M-2B in either P3M or *E. coli* DH5α strains. Considering that p3M-2A could improve the ciprofloxacin resistance of the strain even in the absence of *qnrD*, we speculated that this plasmid may have specific regulatory functions. Thus, we measured the expression level changes of *qnrD* in the presence or absence of p3M-2A using qRT-PCR (Figure 2C,D). The expression level of *qnrD* in P3M and P3M-D2A showed little difference in the absence of ciprofloxacin (Figure 2C). As the concentration of ciprofloxacin increased, the expression level of *qnrD* in both strains increased to different degrees; *qnrD* expression in P3M-D2A was apparently lower than that in the wild-type strain, and the difference became more obvious as the concentration increased. Similarly, the expression of *qnrD* showed the same changing trend in *E. coli* DH5α transformants containing p3M-2B and p3M-2A2B (Figure 2D). These results indicated that p3M-2A played a positive regulatory role in the expression of *qnrD* in p3M-2B, that is, the higher the ciprofloxacin concentration in the environment, the more obvious the regulatory effect of p3M-2A.

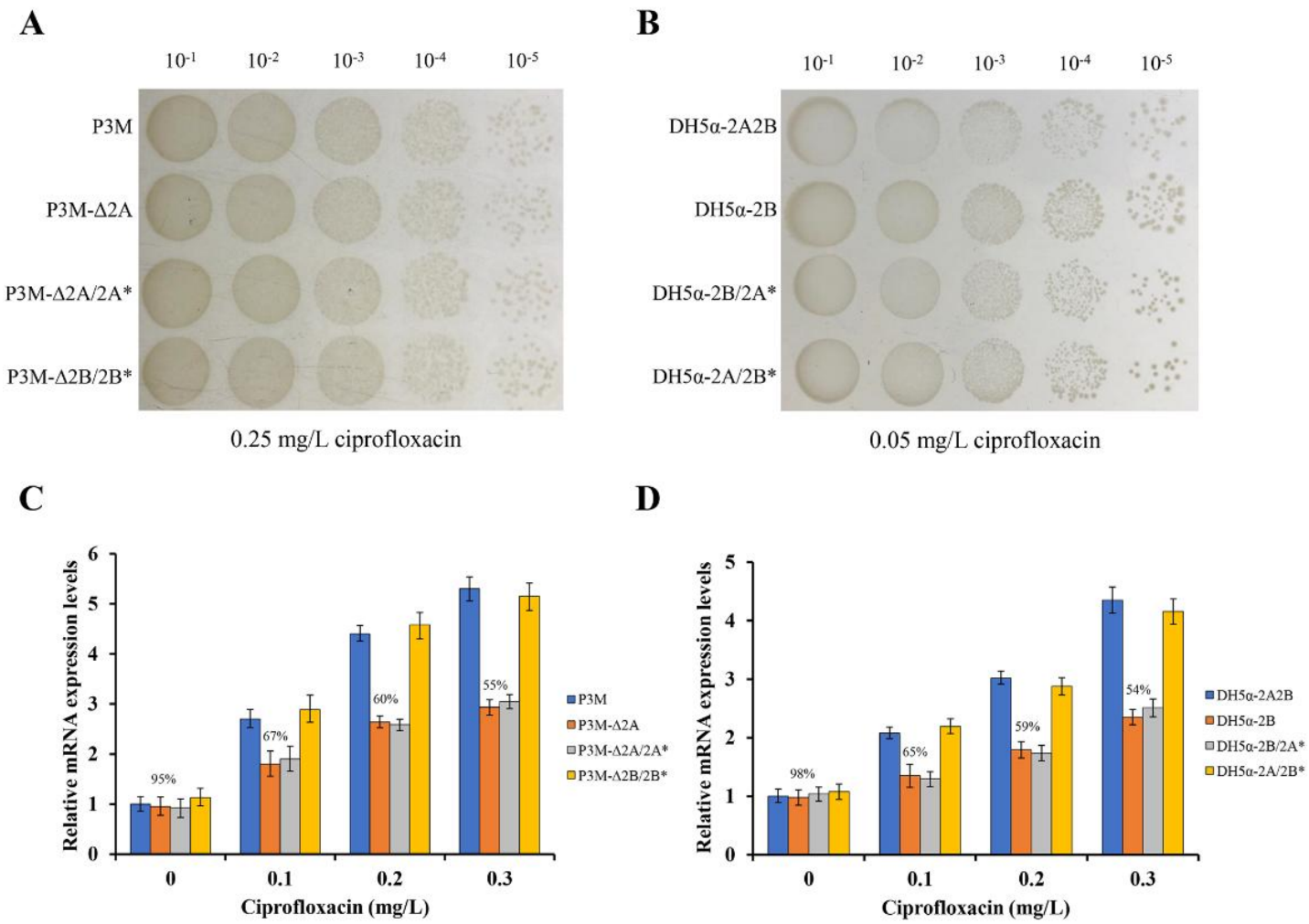

Figure 2. (**A**) Spot growth assays of wild-type (WT) P3M, p3M-2A deleted strain (P3M-Δ2A), p3M-2A* complemented strain (P3M-Δ2A/2A*), and p3M-2B* complemented strain (P3M-Δ2B/2B*) on LB agar in the presence of 0.25 mg/L of ciprofloxacin. (**B**) Spot growth assays of DH5α transformant containing both plasmids (DH5α-2A2B), DH5α transformant containing p3M-2B (DH5α-2B), DH5α-2B strain complemented with p3M-2A* (DH5α-2B/2A*), and DH5α-2A strain complemented with p3M-2B* (DH5α-2A/2B*) on LB agar in the presence of 0.05 mg/L of ciprofloxacin. (**C**) Expression of *qnrD* in P3M, P3M-Δ2A, P3M-Δ2A/2A*, and P3M-Δ2B/2B* with different ciprofloxacin concentrations. (**D**) Expression of *qnrD* in DH5α-2A2B, DH5α-2B, DH5α-2B/2A*, and DH5α-2A/2B* with different ciprofloxacin concentrations.

Since the sequence of *ORF2–ORF3* in p3M-2A shares relatively high identity with that of p3M-2B, while *ORF1* does not (Figure 1B), we speculated that *ORF1* might play a certain regulatory role in *qnrD* expression. Hence, we constructed a new p3M-2A plasmid deleting *ORF1* (p3M-2A*) and transferred it into P3M-Δ2A and DH5α-2B to verify the effect of *ORF1*. As shown in Figure 2A and 2B, the new plasmid p3M-2A* did not affect the normal replication of plasmid p3M-2B in P3M-Δ2A and DH5α-2B, and *qnrD* expression in the transformants was subsequently detected. As expected, p3M-2A* failed to restore the expression of *qnrD* to the wild-type level, but the expression was similar to that of the p3M-2A-deficient strain (Figure 2C,D). These results indicated that *ORF1* in P3M-2A was key to regulate *qnrD* expression, as p3M-2A without *ORF1* could not play its important regulatory function.

2. Phylogenetic Analysis of qnrD-Carrying Plasmids

By analyzing all the *qnrD*-carrying plasmids reported so far, we found that almost all of them were harbored by bacteria isolated from common environmental “reservoirs” like human and animal intestine, urinary tract, feces, water body, etc. 47 *qnrD*-carrying plasmids have been reported to date, of which most of them were isolated from Enterobacteriaceae, with the genus *Proteus* accounting for a relatively large proportion.

Almost all *qnrD*-carrying plasmids reported to date can be roughly divided into 2.7-kb and 4.3-kb categories according to their size. Interestingly, the p3M-2A plasmid in this study was about 2.7 kb in size, although it did not carry *qnrD*. The size of the p3M-2B carrying qnrD was 5.9 kb, and thus it did not comply with the above classification characteristics. In addition, we also found other six special cases that did not conform to the size rule: KVHS-001 (6.9 kb), KVHS-002 (8.1 kb), KVHS-003 (9.4 kb), KVHS-004 (6.2 kb), pOA8916 (2.0 kb), and pMB18 (5.2 kb) (Table S2). In order to further understand the genetic relationship between these *qnrD*-carrying plasmids, a neighbor-joining phylogenetic tree was constructed. As shown in Figure 3, plasmids of the same category tend to be more closely related to each other, while plasmids isolated from *Proteus* were dispersed and could be found in each clade, further illustrating the important function of *Proteus* species as disseminators in the phylogenetic evolution of *qnrD*-carrying plasmids.

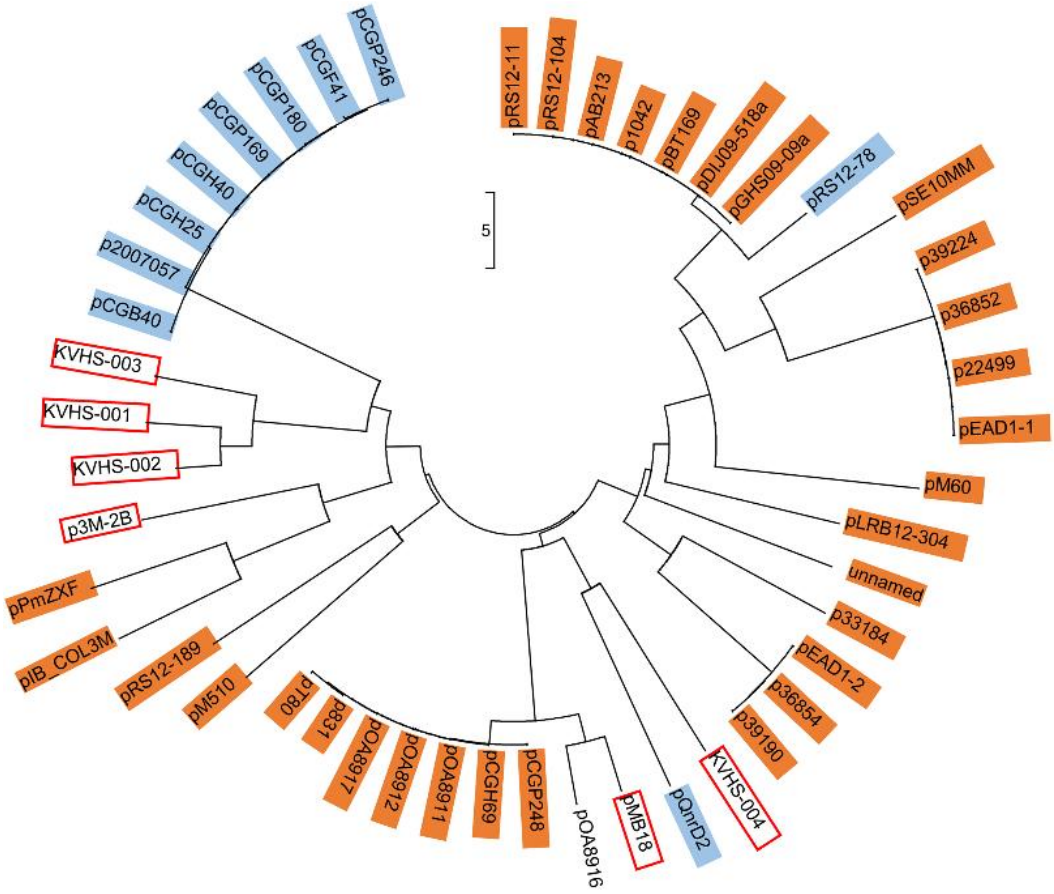

Figure 3. Neighbor-joining phylogenetic tree of p3M-2B with other reported *qnrD*-carrying plasmids. Plasmids of 2.7 kb or 4.3 kb are highlighted in orange or blue, respectively. Plasmids larger than 4.3 kb are marked with red

boxes. The evolutionary history was inferred using the neighbor-joining method. The optimal tree with the sum of branch length of 102.98104110 is shown. The tree is drawn to scale, with branch lengths measured in the same units as those of the evolutionary distances used to infer the phylogenetic tree. The evolutionary distances were computed using the Maximum Composite Likelihood method and are expressed as the number of base substitutions per site. The analysis involved 49 nucleotide sequences. The codon positions included were 1st + 2nd + 3rd + Noncoding. All positions containing gaps and missing data were eliminated. There were a total of 645 positions in the final dataset.

3. Possible Formation Process of p3M-2B

Due to the relatively large size of p3M-2B compared with the 2.7 and 4.3 kb *qnrD*-carrying plasmids, we hypothesized that it may have a specific formation process. We first focused on the other four plasmids isolated from *P. vulgaris* strains which were different in size and made sequence alignments. As shown in Figure 4, *ORF1* (*qnrD*)*-4* of p3M-2B was completely conserved in these four *qnrD*-carrying plasmids, with sequence identity up to 100%. Besides, the 2683-bp plasmids p36852 and pEAD1-1 appeared to be exactly composed of *ORF1–4*, implying that these four conserved genes of p3M-2B are the most conserved genes of the *qnrD*-carrying plasmids, necessary for their normal function.

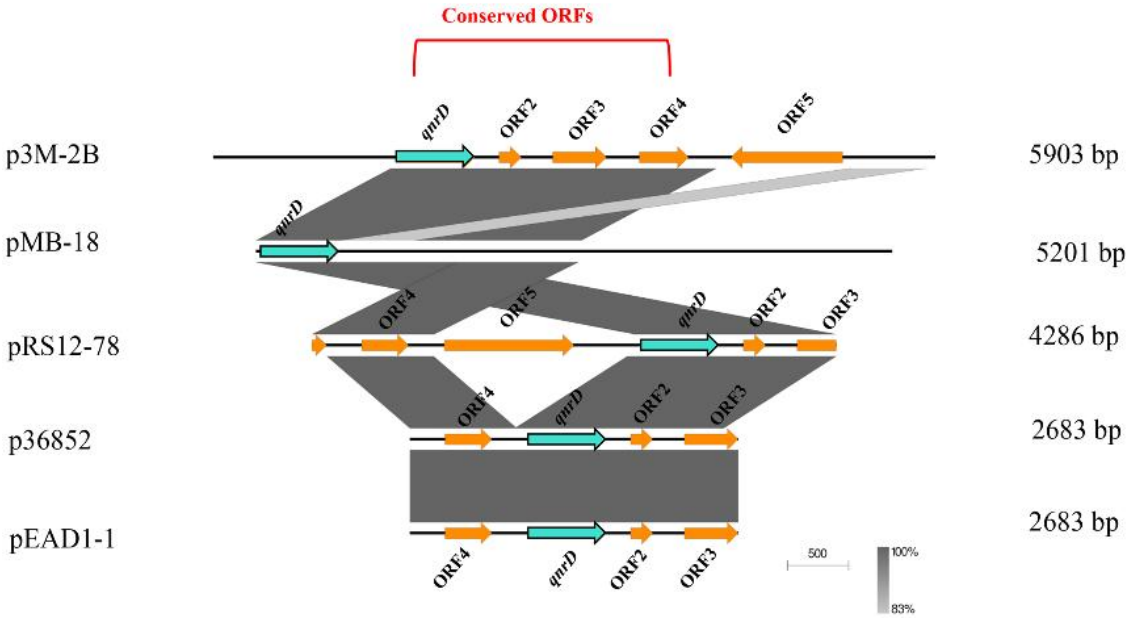

Figure 4. Linear comparison of p3M-2B with other closely related *qnrD*-carrying plasmids isolated from *P. vulgaris* strains.

Subsequently, the p3M-2B plasmid sequence was analyzed with RepeatAround, a Windowsbased software tool designed to find repeats from 3 bp to 64 bp of length in circular genomes. We found that there were four pairs of DR or inverted repeats (IR) in p3M-2B (Figure 5), and it was notable that the sequence length between DR-C1 and -C2 was precisely 2683 bp, which fitted into the category of 2683-bp *qnrD*-carrying plasmids. In particular, the sequence between C1 and C2 corresponded exactly to *ORF1–4*, which appeared to be the most conserved and

essential genetic component of qnrD-carrying plasmids for their proper function (Figure 4). It has been reported that DNA recombination mediated by DR regions is a major cause of genome plasticity, so it is conceivable that the DR present in p3M-2B would have a similar function. We hereby supposed that the 5903-bp p3M-2B may be originally derived from a 2683-bp plasmid, and DR-C1 and C2 play an important role in this process.

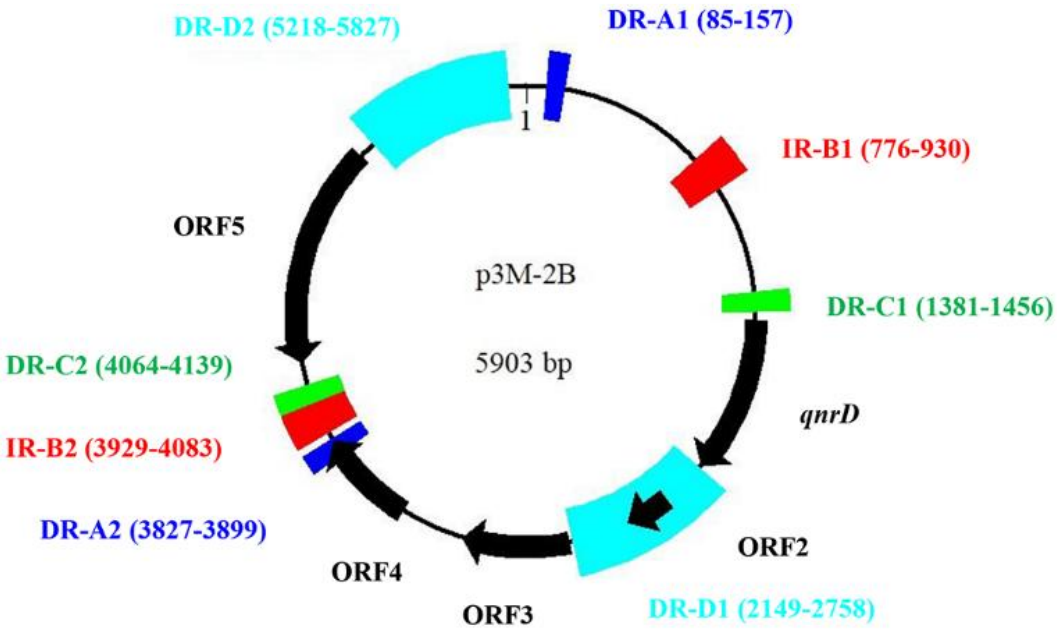

Figure 5. Graphical map of p3M-2B including direct repeats (DR) and inverted repeats (IR). Motifs of the same color represent a pair of DR or IR regions.

To test the above hypothesis, a new 2683-bp p3M-2B plasmid without *ORF5* (p3M-2B*) was constructed, and its stability and *qnrD* expression in the transformants P3M-Δ2B/2B* and DH5α-2A/2B* (Figure 2) were tested. Just as we expected, p3M-2B* was stable in the transformed strains (Figure 2A,B), and the expression of *qnrD* at different ciprofloxacin concentrations was not affected by *ORF5* deficiency (Figure 2C,D). These results further indicated that *ORF1–4* in *qnrD*-carrying plasmids is a very conserved backbone, and *ORF5* in p3M-2B, which appears to be an acquired exogenous sequence, does not affect the normal replication process and further quinolone resistance.

To further explore whether this is applicable to all larger *qnrD*-carrying plasmids, we made sequence alignments of the DR-C region in p3M-2B with similar regions in other reported *qnrD*-carrying plasmids. As shown in Figure 6, we found that although all plasmids contained DR regions sharing high sequence identity with DR-C, sequences varied slightly among different plasmids. The sequence with high identity to DR-C was present only in one site in the 2.7-kb plasmids, located upstream of *qnrD* (Figure 6A). It should be noted that although p3M-2A does not carry *qnrD*, it was also included in Figure 6A because it appeared to be in the 2.7-kb plasmid category and share high sequence identity with DR-C. Likewise, all 4.3-kb plasmids contained only one site identical with DR-C, with the exception of plasmid pRS12-78, containing two DR-C regions at different positions (Figure 6B). As shown in Figure 6C, among all plasmids larger than 4.3 kb, only pMB18 appeared to be consistent with p3M-2B, with two different DR regions (DR-C1 and C2), while only one DR-C was found in the four larger *qnrD*-carrying fragments isolated from *Salmonella*, which was unexpected. Plasmid pOA8916, smaller than 2.7 kb, contained one spot of DR-C

upstream of *qnrD* as well (not shown).

In summary, among all the *qnrD*-carrying plasmids analyzed, only p3M-2B, pMB18, and pRS12-78 presented two different DR regions, and the sequence lengths between them resulted to be exactly 2683 bp, containing *ORF1–4*. Notably, these three plasmids were isolated from *P. vulgaris* strains, which hints at the important host role of *P. vulgaris* in plasmid propagation.

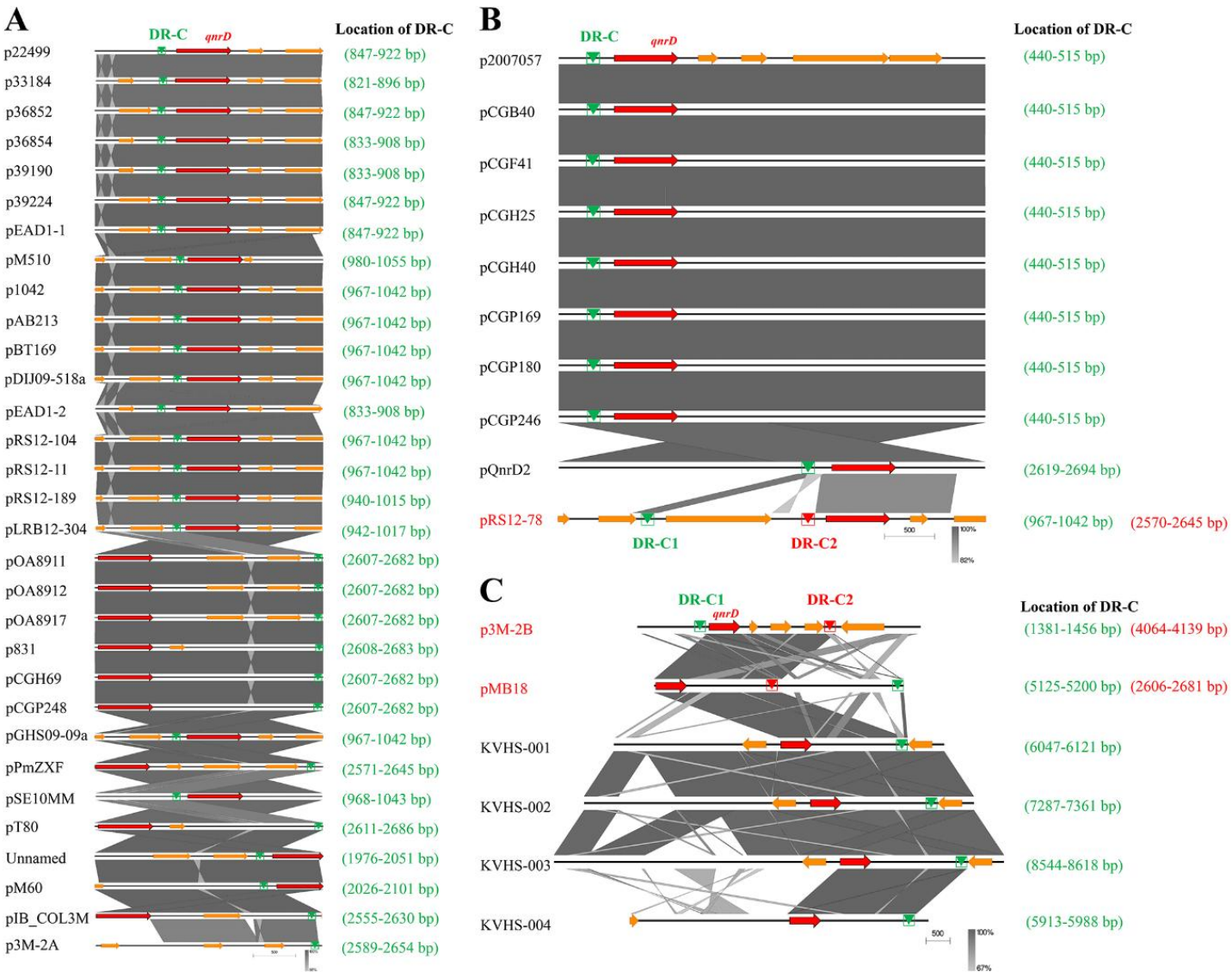

Figure 6. Comparative linear maps of *qnrD*-carrying plasmids of (**A**) 2.7 kb, (**B**) 4.3 kb, and (**C**) larger than 4.3 kb; *qnrD* and other predicted coding sequences (CDS) are denoted by red and orange arrows, respectively. The size of the arrows is to scale. The green and red triangles represent the regions sharing high sequence identity with DR-C in p3M-2B.

Based on the structural characteristics of the above three plasmids, we propose a potential model for the development of larger *qnrD*-carrying plasmids like p3M-2B (Figure 7). The p3M-2B backbone with an initial size of 2.7 kb contains DR-C region about 35–115 bp upstream of *qnrD*. The exogenous sequence containing DR-C at both ends in the adjacent environment may undergo homologous recombination with the DR-C region in p3M-2B

(2.7 kb) and thus be integrated to turn into a new *ORF*. Ultimately, a novel plasmid p3M-2B of 5.9 kb is formed.

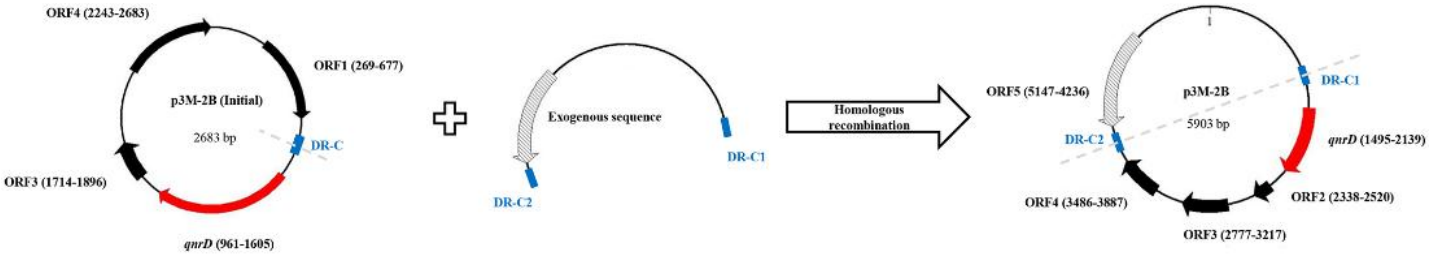

Figure 7. Possible model for in vivo formation of 5903-bp p3M-2B.